



Conceptual Design of a Solar-Powered Winged Hybrid Airship for Agricultural Purposes

Rithik R. Nambiar* and Pranav Gupta†
Indian Institute of Technology Bombay, Mumbai, India-400076

Manikandan M ‡
Manipal Institute of Technology, Manipal Academy of Higher Education, Karnataka, India-576104

Agriculture has been fundamental to human sustenance since ancient times. As the need for food production continues to escalate, researchers have been exploring methods to enhance yield while minimizing resource usage and environmental impact. In light of the rising worldwide population, there is an anticipated surge in food demand, and precision farming offers a hopeful remedy to satisfy this demand. This study presents a conceptual design and sizing of a winged hybrid airship for agricultural purposes. The airship is designed to provide a cost-effective and eco-friendly solution for crop monitoring and fertilization. The design process includes the determination of the payload capacity, cruise altitude, range, and endurance of the airship. The propulsion system is a combination of solar panels and electric motors. The airship's lifting mechanism is achieved through the use of helium and aerodynamic lift. The results show that the airship has the potential to carry a payload of up to 30 kg with an endurance of 24 hours. The proposed design offers a significant improvement in efficiency compared to traditional crop monitoring methods.

I. Nomenclature

AR	=	Aspect Ratio
b	=	Wing span
C_D	=	Drag coefficient
C_L	=	Lift coefficient
H_{opr}	=	Operational altitude
I_{solar}	=	Irradiance
L_{net}	=	Static lift
l	=	Length of Airship
LTA	=	Lighter than air
S	=	Surface area
UAVs	=	Unmanned aerial vehicles
V_{env}	=	Volume of the envelope
V_{opr}	=	Operational velocity
W	=	Weight
FR	=	Fineness Ratio
gsm	=	Grams per square metre
S_{fin}	=	Surface area of fins
C_r	=	Root chord
c_t	=	Tip chord
b_t	=	Tailspan
a	=	Profile cylinder ratio
D_{max}	=	Maximum diameter

*Project Research Assistant, Department of Aerospace Engineering, AIAA Non-Member.

†Project Research Assistant, Department of Aerospace Engineering, AIAA Non-Member.

‡Senior Assistant Professor, Department of Aeronautical and Automobile Engineering, AIAA Non-Member

II. Introduction

THROUGHOUT human history, agriculture has played a crucial role in sustaining civilizations. From hunter-gatherers to settled communities, farming has been the backbone of human survival. In India, agriculture has been the primary source of livelihood for centuries, and the sector has been witnessing substantial growth over the past few years due to increased investment. In fact, the agricultural sector in India has become one of the most prominent and revenue-generating sectors in recent times. According to the World Bank, agricultural land accounted for 60.22% of the country's total land area in 2020. With the world's population projected to reach 9.7 billion by 2050, there will be a need for a 70% increase in global food production [1]. Developing countries like India and China, which have the largest areas of arable land for agricultural purposes, will play a vital role in meeting this demand. To address the growing need for food production, scientists have been researching ways to maximize output while minimizing input and reducing environmental impact [2]. Precision agriculture (PA) has emerged as a promising solution to achieve these objectives. The main goal of PA is to optimize crop production while minimizing the use of harmful chemicals and promoting a healthier environment for humans. Despite the numerous benefits of PA, there are still some key challenges that need to be addressed [3]. For instance, there is a need for appropriate decision-support systems and environmental auditing. However, innovations in technology have greatly accelerated the transition to precision agriculture. One such innovation is the development of hybrid airships, which have high endurance flight capabilities at high altitudes. These airships have numerous applications, ranging from military surveillance missions to commercial and strategic applications such as wireless broadband telecommunications, digital broadcasting, coastal surveillance, remote sensing, and GPS-augmented navigation systems. With the growing global population, there will be an increasing demand for food production, and precision agriculture presents a promising solution to meet this demand. Innovations in technology, such as hybrid airships, will also play a vital role in advancing agriculture and meeting the world's food requirements.

III. Literature Review

The rise of precision farming using UAVs gives great advantages to farmers worldwide. 80% of the commercial UAV market is expected to be captured by Agriculture UAVs and has the potential for many job openings [4]. In the Indian state of Maharashtra, UAVs are actively used for creating maps and irrigating farmlands. Farmers study the prediction of harvests, take action at the early stages, classify crop types, and plan harvesting, and pest control [5]. Currently, monitoring of agricultural lands is carried out using helicopters, airplanes, and satellites which are expensive and time-consuming. UAVs have made life easier for farmers by being cheaper and faster. UAVs equipped with optical and satellite navigation provide accurate positioning in a given area. A few examples of such drones are shown in Figure 1 and 2.



(a) Precision Hawk Lancaster [6]



(b) Sunseeker duo [7]

Fig. 1 Fixed Wing UAVs used for agricultural application



Fig. 2 Multi-Rotor UAVs used for agricultural application

All of these are possible today due to the huge leap in battery technologies since power sources are one of the main drone components. The design solutions are found from their charge rate, operation duration, weight, and durability. Drones currently can fly within a few hours and load capacity to carry the weight of the equipment on the drones [10]. However, even with such capabilities, it is impossible to use them in hard-to-reach areas of the cultivating land. The common disadvantage of these devices is the high cost of equipment and operation as well as low efficiency. For example, in case of a fire hazard airplanes and helicopters constantly have to refuel the water, fly up to the designated site and fly away for refueling during which a stronger fire flares up [11]. In Russia and abroad, a new class of hybrid aircraft has appeared combining the principles of an airship, an airplane, and a helicopter [4]: In the USA - P-791 of Lockheed Martin [12], and in England - Skyship [13]. In China, the French company Flying Whales, together with the Chinese state aircraft company General Aircraft Co., Ltd, are building a plant for LCA60T rigid airships with a carrying capacity of 60 tons, filled with helium as shown in Figure 3



Fig. 3 LTA systems used for agricultural purposes

Airships are becoming popular in agriculture for crop monitoring, mapping, and spraying. These systems offer farmers benefits such as high-resolution crop images, precise spraying capabilities, and valuable data on soil moisture and temperature, which can help increase crop yields, reduce waste, and minimize the use of chemicals. However, to ensure the safety and effectiveness of their use, regulations must be in place. Despite these advantages, airships were initially overlooked until they returned to the picture due to their remarkable benefits as a low-cost and environmentally friendly mode of transportation. Figure 4 illustrates the applications of LTA systems in agriculture. By utilizing a hybrid configuration, airships can stay in a specific location for longer periods with minimal fuel consumption and carry heavy loads better than other UAV configurations due to their lesser reliance on the dynamic lift.

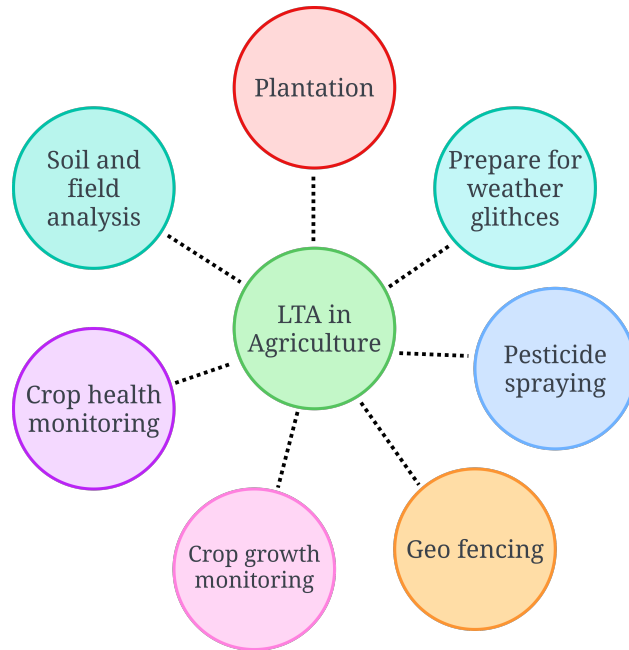


Fig. 4 Applications of LTA systems in Agriculture

Winged hybrid airships generate dynamic lift that can be modulated to keep the airship stable throughout the mission. These airships have massive differences compared to conventional airships in general configuration, principles of lift generation, aerodynamic configurations, etc. They have more acceptable ground handling capabilities and are more aerodynamically efficient compared to conventional airships. Hybrid airships have the combination of aerodynamic lift and buoyancy lift which enables them for longer sustainable flight for longer durations. Table 1 provides a comparison of various UAVs and airships used in different sectors, including agricultural UAVs such as the DJI Matrice 300 RTK [8], and Yamaha RMAX [9]. It includes information on the type, length, weight, endurance, payload capacity, and operational altitude of each vehicle.

Table 1 Comparison data of various Agricultural UAVs and LTA systems

UAV/Airship	Configuration	Length (m)	Payload Mass (kg)	Endurance	Total Weight (kg)	Operational Altitude (m)
P4 Multispectral	Quadcopter	0.29	0.64	27 mins	1.37	122
Agras T16	Octacopter	1.82	16.5	22 mins	16	2.5
DJI Matrice 300 RTK	Quadcopter	0.887	2.7	Up to 55 mins	3.6	7000
BIRDIE	Quadcopter	0.6	1.5	Up to 60 mins	2.5	100
Yamaha RMAX	Helicopter	3.35	28.6	Up to 90 mins	210	300
Precision Hawk Lancaster	Fixed Wing	1.37	1.36	Up to 50 mins	2.7	122
Sun Flyer	Fixed Wing	8.5	240	Up to 5 hours	227	4572
Sunseeker Duo	Fixed Wing	22	40	Up to 12 hours	52	15240
AtlantikSolar	Fixed Wing	6.8	5	Up to 12 hours	25	6000
P-791	Hybrid Airship	74.4	22680	Up to 3 days	241000	6096
Sky ship 600	Rigid Airship	53.3	2300	Up to 10 hours	9072	2133
LCA60T Rigid Airship	Rigid Airship	60	2000	Up to 6 hours	25000	3000

Based on a careful examination of the literature and a comparative study between agricultural drones and hybrid airships, it is obvious that the latter outperforms the former in terms of endurance, maximum height, and payload capacity. Hybrid airships have the capacity to function at distinctive heights and have more prominent endurance, resulting in longer flight times and larger land range coverage. Moreover, their capacity to transport huge cargoes makes them a perfect choice for agricultural use. Therefore, our mission is to investigate and execute the use of winged hybrid airships as a more profitable alternative to UAVs within the agricultural industry, particularly for large operations that require broad coverage. From the conducted literature analysis it is apparent that in order for our vehicle to have competitive performance parameters the endurance and payload mass must be maximized. The plan for implementing winged configuration is to reduce the reliance on buoyancy lift on the system. This configuration also helps to install solar panels for additional power requirements on the wing. This paper also concentrates on developing a technique to maintain the static lift of the system when the payload decreases throughout the flight.

IV. Mission Overview

The take-off of a winged hybrid airship typically involves an initial climb phase that is facilitated by the propulsion system onboard. This is followed by the cruise phase, which typically accounts for 60-70% of the mission duration. During this phase, the airship carries out its primary mission objectives, such as surveillance or spraying fertilizers. The cruise phase is particularly important for analysis, as it is the period during which the airship's performance and efficiency are most critical. After completing the mission objectives, the airship then enters the descent phase, which involves a controlled reduction in altitude and airspeed in preparation for landing. Landing is typically the final phase of the mission and requires careful planning and execution to ensure the safe and efficient handling of the airship. Throughout all phases of the mission, careful attention must be paid to the airship's performance and stability, as well as any external factors such as weather conditions, to ensure a successful and safe flight.

A. Mission Requirements

Based on the conducted literature analysis certain mission requirements were decided upon to give our vehicle competitive performance parameters which are summarised in Table 2.

Table 2 Mission Requirements

Parameter	Value
Vehicle Weight	≤ 250 kg
Takeoff and Land	Within 500 m @ Sea Level Conditions
Payload Weight	30 kg
Payload Power Consumption	100 W
Atmosphere	International Standard Atmosphere (ISA)
Endurance	24 hours

B. Mission Profile

The mission profile is the path the vehicle takes while executing its mission. The below-mentioned diagram shows the different mission profile segments taken by the aircraft. The mission profile was found to be predominantly cruise and turn flight. Thus, the design process was conducted to optimize the performance parameters, especially during those stages of flight. The design also incorporated a safe margin for the aerodynamic forces which would help mitigate the miscellaneous forces and moments encountered by the vehicle during its entire mission ensuring durability and safety of the vehicle. The mission profile for the proposed vehicle is shown in Figure 5.



Fig. 5 Mission Profile of the proposed vehicle

C. Design Overview

A comprehensive review of the mission requirements led to the conclusion that an airship was a suitable option for meeting the specified criteria. However, meeting the substantial endurance requirements using internal combustion engines and fossil fuels was deemed unfeasible. Thus, a solar-powered electrical propulsion system was selected, with solar panels mounted on the top surface of the airship's envelope to optimize efficiency. To further improve efficiency, a modified GNVR envelope shape was chosen, resulting in a flatter upper surface that would enhance the performance of the solar panels by reducing drag. Additionally, the airship was designed with a rectangular wing and X-tail configuration, aimed at enhancing the stability and control of the aircraft to ensure safe and effective mission performance. The methodology utilized to design this airship, as well as the results obtained, are discussed in detail in the subsequent sections.

V. Methodology

Designing a solar-powered, winged hybrid airship requires a multidisciplinary approach that encompasses six essential submodules. These include:

- a) **Aerostatics** is a critical component in the design and operation of LTA systems. This sub-module is specifically tailored to calculate the net static lift generated by the LTA vehicle, taking into consideration various parameters of the lifting gas used. These parameters may include gas density, volume, pressure, temperature, and humidity, among others. The net static lift is a crucial factor in determining the LTA vehicle's ability to remain buoyant and achieve stable flight. By accurately estimating the net static lift, the aerostatics sub-module enables designers and operators to optimize the LTA vehicle's performance and ensure safe and reliable operation.
- b) **Aerodynamics** is an essential tool for designing and evaluating the performance of the wings of a winged hybrid airship. This sub-module enables designers to estimate the required size and geometry of the wing, based on the

aerodynamic forces and moments acting on the airship during flight.

By taking into account the airship's weight, speed, altitude, and other key parameters, the aerodynamic sub-module provides a starting point for determining the optimal wing size and configuration. This includes factors such as the wing area, aspect ratio, taper ratio, and sweep angle, among others.

Furthermore, the aerodynamic sub-module can also be used to evaluate the aerodynamic performance of different wing designs, enabling designers to compare and select the most efficient and effective option for the winged hybrid airship.

- c) **Geometry** which deals with the design of the airship's envelope, fins, and wings. The selection of an appropriate airfoil and conducting trade studies to optimize the aspect ratio and C_{D0} are critical in this sub-module.
- d) **Drag** which involves the analysis of the vehicle's drag characteristics, including parasitic drag and induced drag. This sub-module helps in determining the vehicle's required power input.
- e) **Propulsion** which focuses on the design of the vehicle's propulsion system, including the size and power output of solar panels.
- f) **Weight Estimation** which is concerned with determining the vehicle's weight distribution and the corresponding free lift, essential for stable flight.

Overall, the successful design of a solar-powered, winged hybrid airship is a complex process that involves a thorough consideration of multiple factors. The six sub-modules of aerostatics, aerodynamics, geometry, drag, propulsion, and weight estimation are the building blocks of this process and are integral to creating an efficient and effective airship. Figure 6 presented depicts a framework for creating a hybrid airship with wings that is powered by solar energy.

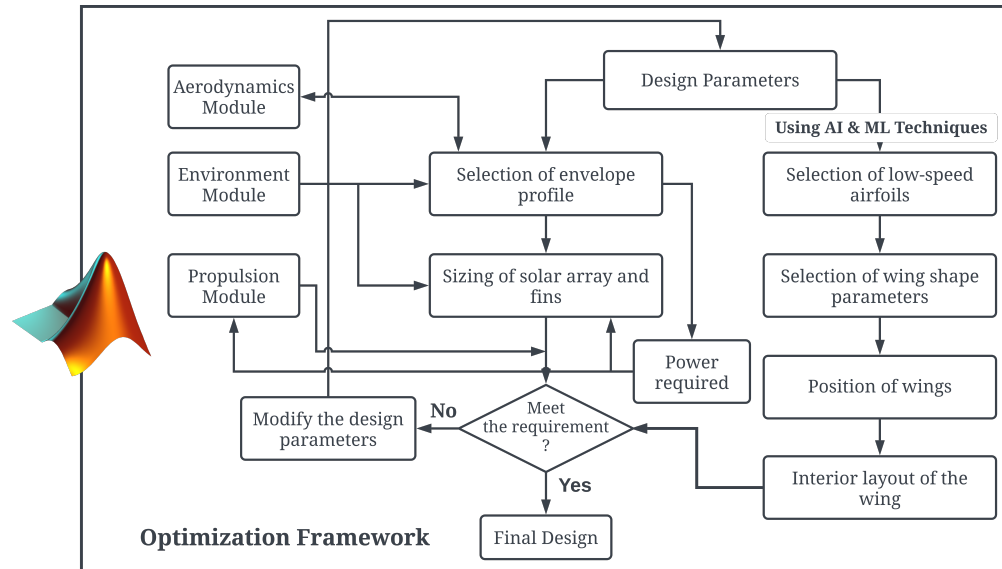


Fig. 6 Optimization framework

A. Envelope Profile Selection

A critical study of the above-mentioned mission requirements revealed that an airship would be the most suitable candidate for meeting the specified requirements. Since the endurance requirements were very large, it was considered almost impossible to meet them using any power plant based on internal combustion engines and fossil fuels. It was decided to go for a solar-powered electrical propulsion system, powered using solar panels mounted on the top surface of the airship envelope. The efficiency and overall performance of an airship are highly influenced by the form and size of its envelope, which impacts the drag pressure and buoyant lift. Various envelope shapes are feasible, such as the oblate spheroid, LYNX, Zhiyuan, GNVR, and Modified GNVR, the latter being a popular choice due to its streamlined design and ease of fabrication.

Upon careful analysis of the above-mentioned mission requirements revealed that an airship would be one of the viable configurations for meeting the specified requirements. Based on the analysis of the literature and the proposed endurance of the airship, solar-powered electric propulsion was deemed appropriate for this mission where the solar

panels would be mounted on the top surface of the airship envelope. To reduce the effects of drag for equivalent volume a modified GNVR envelope shown in Figure 7 was selected which resulted in a comparatively flatter upper surface to increase the solar cell efficiency.

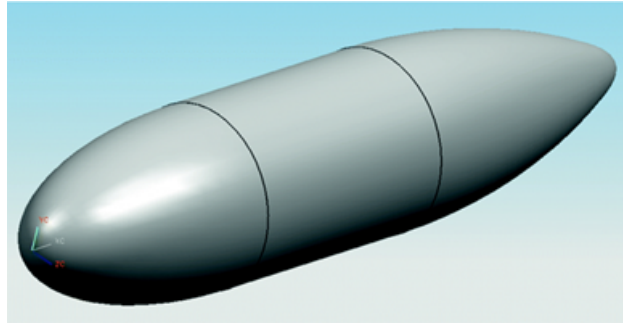


Fig. 7 Modified GNVR envelope [15]

B. Envelope Geometry Parameters

After the initial selection of the envelope profile, the next step in the design process is to input an arbitrary value of maximum diameter to calculate the various envelope geometry parameters. To do this, it is crucial to understand the relationships that govern the dimensional properties of the envelope.

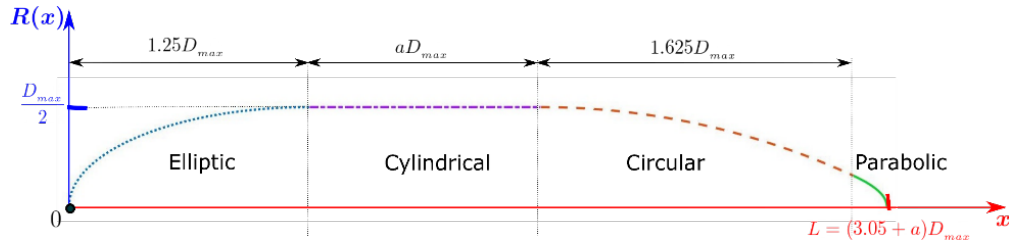


Fig. 8 Modified GNVR shape

$$V_{env} = \left(\frac{\pi a}{4} + 1.5 \right) D_{max}^3 \quad (1)$$

$$SA_{env} = (\pi a + 7.5) D_{max}^2 \quad (2)$$

For instance, for the modified GNVR envelope profile shown in Figure 8, Equations 1 and 2 can be used to calculate the volume and surface area, respectively. These equations consider various factors such as the length, width, and maximum diameter of the envelope. By using these equations, the designer can determine the optimal dimensions of the envelope to ensure that it meets the requirements of the airship's intended mission profile.

C. Estimation of Aerostatic Lift

In the context of the Precision Agriculture application for this vehicle, operating in close proximity to the ground is a critical requirement. This is because the airship is intended to either map the field or spray pesticides, tasks that require a near-surface operation. To facilitate this, helium is the preferred lifting gas to be used inside the airship envelope. This is due to several reasons. Firstly, helium is an inert gas, making it safe and easy to use. More importantly, it is non-combustible, which eliminates any potential fire hazard associated with other gases.

For the purpose of calculating the net static lift L_{net} , it is assumed that there is a complete thermal equilibrium between the helium gas inside the airship and the ambient atmosphere. This is due to the long duration of deployment of the airship. The ambient temperature and pressure of the helium gas are considered to be the same as that of the surrounding air, and their values are obtained using the ISA charts. By using Equation 3 given by Taylor, the net static lift L_{net} can be calculated. This equation considers the difference in density between the ambient air and helium gas

inside the envelope, the volume of the envelope, and the gravitational constant. By accurately calculating the net static lift L_n , the designer can ensure that the airship has the necessary lift to operate at a near-surface level and complete its intended mission.

$$L_{net} = (\rho_{Air} - \rho_{He}) \cdot V_{env} \cdot g \quad (3)$$

D. Wing Design

A conventional monoplane with a rectangular planform was decided upon befitting lift and stall characteristics in the low-speed regime. Rectangular planform also possesses an edge over other wing designs due to its simplicity and ease of construction and assembly. A mid-wing configuration was selected owing to its increased lateral stability, better ground clearance, and reduced drag as the wings are mounted closer to the CG thereby not obstructing the airflow over the airship envelope allowing a more streamlined design to be generated. This configuration would also facilitate easy access to the wing and supplies from the payload bay, thus giving it an operational advantage congruous with the mission requirement.

The wing sizing was executed in compliance with the mission requirements. The wing was proposed to be sized in such a manner that would result in the generation of high lift force enabling the aircraft to carry maximum payload whilst maintaining the structural integrity of the wing.

1. Airfoil Design

The airfoil is regarded as the heart of the wing's design as it influences the major attributes of the vehicle namely its performance and stability. For the given mission, the wing was designed in such a manner as to maximize the amount of payload it can carry. For these reasons, a high-lifting airfoil was desired with appropriate stall characteristics. The team analyzed a plethora of airfoils on the *XFLR-5* software [16] at various Reynolds numbers, using Vortex Lattice Method (VLM) and Computational Fluid Dynamics (CFD). The values of the lift, drag, and moment coefficients were obtained at various angles of attack upon analysis. In order to perform the given mission successfully, We identified the necessity of selecting an airfoil that exhibits a high C_{l_0} value to generate lift for the payload, while simultaneously maintaining a desirable pitching moment coefficient to ensure the stability of the aircraft. The airfoil that met all the objectives was Selig 1223 airfoil.

2. Aspect Ratio Selection

The aspect ratio of the wing is a fundamental parameter that influences stability, maneuverability, induced drag generated, and bending moment. A high aspect ratio decreases the induced drag over the wing at the cost of increased bending moment. A low aspect ratio wing has a lower bending moment but compromises on aerodynamic characteristics. Initial studies suggested that aspect ratios between 8 and 10 were feasible and provided a favorable combination of the above characteristics. Figure 9 shows the variation of induced drag with aspect ratio.

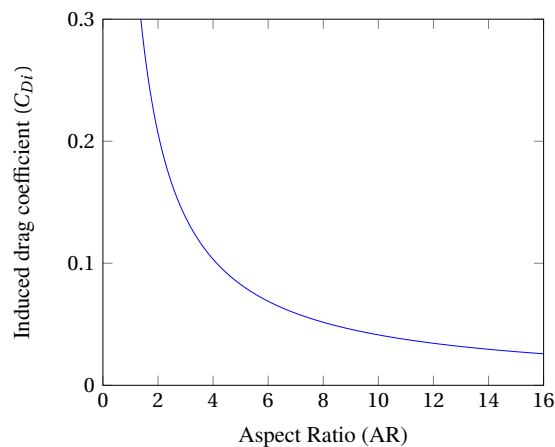


Fig. 9 Variation of Induced Drag Coefficient with Aspect Ratio

E. Initial Tail Sizing

In determining the appropriate size for the tail of the airship, we conducted an extensive analysis of multiple airships to establish a baseline for comparison. This analysis included performing a regression analysis on the parameters of these airships to identify patterns and trends. Based on this analysis, we found that the most used tail configurations for airships are the "X," "+," and "inverted Y" configurations. After careful consideration, we decided to use the "X" configuration in our proposed airship design.

We selected the "X" configuration primarily because of its larger size compared to the other configurations, which provides greater stability and control during flight. Additionally, the "X" configuration allows for easier ground handling of the airship, which is an important consideration for efficient operations. The side-view of the fin is shown in Figure 10. The design parameters of the fins are listed in Table 3.

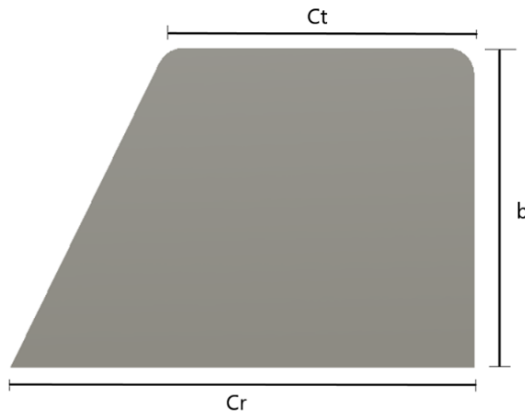


Fig. 10 Front view of the fin

Table 3 Fin Parameters

Fin Parameter	Formula	Value
Area Ratio	S_{fin}/S_{env}	0.0594
Aspect Ratio	$4b^2/S_{fin}$	0.6585
Span to chord ratio	b/C_r	0.5625
Taper ratio	C_t/C_r	0.7083
Location Ratio	L_{fin}/L_{env}	0.8

F. Payload Bay Design

The vehicle was designed with a specific focus on its ability to carry agricultural supplies and materials, in line with the mission requirements of carrying a 30 kg payload. The payload bay design was approached with this agricultural purpose in mind, and various trade studies and box volume analyses were conducted to determine the optimal dimensions for the bay.

It was understood that the payload could be dynamic in nature, and special efforts were taken to ensure that the center of gravity (CG) of the payload bay coincides with the CG of the entire vehicle. This helps to maintain stability and balance during flight, even with a dynamically shifting payload. A ballast is also added to maintain the center of gravity (CG) of the airship and adjust its altitude. The ballast weight can be increased or decreased to change the lift of the airship, allowing it to ascend or descend as needed to ensure the safe delivery of agricultural supplies.

Based on the trade studies conducted and the analysis performed, the dimensions of the payload bay were summarized in Table 4, taking into account the required payload weight and the size and shape of the agricultural materials to be transported. The final dimensions were determined to provide optimal balance and stability while ensuring that the necessary materials could be safely and efficiently transported.

Table 4 Payload Bay Design parameters

Parameter	Value (m)
Length	0.75
Breadth	0.75
Height	0.5

In the process of fabricating the gondola, various materials were evaluated based on their strength and availability. After careful consideration, HDPE was chosen as the material for the gondola. HDPE has a density of $20\text{kg}/\text{m}^3$, and its

mechanical properties make it suitable for the requirements of the gondola.

G. Drag and Power Computation

The total drag of a vehicle can be calculated by summing up the drag generated by each component of the vehicle, such as the drag generated by the airship, the wing, and the solar panels.

$$\text{Total Drag} = \text{Drag}_{\text{airship}} + \text{Drag}_{\text{wing}} + \text{Drag}_{\text{solar panels}} \quad (4)$$

By adding up the drag of each component, we can get the total drag of the vehicle. This information is crucial in the design and optimization of vehicles, as minimizing drag is essential for reducing fuel consumption and improving efficiency. By reducing the total drag of a vehicle, we can increase its speed and range while reducing its energy consumption, resulting in a more sustainable and cost-effective transportation system.

1. Airship Drag

The first step in analyzing the aerodynamics of an object was to determine the volumetric drag coefficient (C_{Dv}), which was calculated using a formula created by Hoerner. This formula takes into account two key parameters: the fineness ratio (the length of the object divided by its diameter) and the Reynolds number (a measure of the fluid flow around the object). By using this formula, we can determine the (C_{Dv}) of an object without needing to consider its specific shape. This is because the formula is independent of the envelope shape, allowing us to compare the (C_{Dv}) of different objects with different shapes.

The (C_{Dv}) is a critical parameter to consider when analyzing the aerodynamics of an object. It measures the resistance that an object experiences as it moves through a fluid, such as air or water. The higher the (C_{Dv}), the greater the resistance and the harder it is for the object to move through the fluid.

$$C_{Dv} = \frac{0.172 \left(\frac{l}{d}\right)^{1/3} + 0.252 \left(\frac{d}{l}\right)^{1.2} + 1.032 \left(\frac{d}{l}\right)^{2.7}}{\text{Re}^{1/6}} \quad (5)$$

Once this coefficient has been determined, it is possible to calculate the envelope drag using the formula given below.

$$\text{Drag} = \frac{1}{2} \rho v^2 \text{Vol}^{2/3} \quad (6)$$

It is also necessary to consider the drag force exerted by various components of the airship, such as the tail, solar panels, gondola, propulsion system, and other miscellaneous elements. To do this, the envelope drag is doubled, based on historical data and trends observed for other airships. By multiplying the envelope drag by a factor of 2, we can obtain a more accurate estimate of the total drag force that the airship will experience. This information is critical for designing an airship that can achieve the desired speed and range, while also minimizing energy consumption and maximizing efficiency.

2. Wing Drag

To analyze the aerodynamic properties of a wing, a model was created using *XFLR-5* software. The software allowed for an analysis of the lift and drag coefficients of the wing design. Based on the dimensions of the wing and its operating velocity, the corresponding Reynolds number was calculated. The Reynolds number is a dimensionless quantity used to predict the flow pattern of a fluid around an object. To determine the 3D drag coefficient of the wing, the Vortice Lattice method was used. This mathematical approach allowed for a comprehensive analysis of the aerodynamic properties of the wing. By analyzing the airflow around the wing, the Vortex Lattice method can predict the drag coefficient of the wing in three dimensions. The combination of *XFLR-5* software, Reynolds number calculation, and the Vortex Lattice method provided a detailed analysis of the wing's aerodynamic properties. This information can be used to optimize the design of the wing and improve its overall performance in real-world applications.

H. Solar Panel Sizing

Our system needs to generate enough power to complete our mission, which includes powering our onboard payload at 100 W in addition to the propulsive power. We evaluated various solar panels and ultimately chose the ASCA® Solar

Panels for their flexibility and ability to easily mount on our airship envelope. However, due to prolonged exposure to solar radiation, these panels need to be padded with insulation material to protect the envelope. We calculated the required solar cell area by determining the total power needed based on the irradiance and cell efficiency and then deciding where to mount the cells on the envelope. The properties of which are enumerated in Table 5.

Table 5 Panel sizing properties

Parameter	Unit	Value
Irradiance	W/m ²	950
Cell efficiency	%	12
Solar panel area density	g/m ²	1000

I. Envelope and tail material selection

Selecting the appropriate material for the envelope and tail is a crucial aspect of designing a product. It is essential to consider factors such as weight, tear resistance, and durability while choosing a material. The selection process must involve a thorough analysis of various available materials to determine the most suitable one for the product's intended use. After a comprehensive review of available materials, we have chosen to use 110 gsm LDPE for the envelope and 200 gsm LDPE for the tail. These materials have several beneficial properties, including being lightweight and having high tear resistance, making them ideal for our product. LDPE is a low-density polyethylene material known for its toughness, flexibility, and ability to withstand various environmental conditions.

An additional factor of 5% was added to the envelope's total surface area, and 3% was added to the fin's total surface area, to account for the additional material used in joints and patches. These factors help to ensure that the design of the airship's envelope and fins takes into account the necessary material margins and allows for a safe and reliable operational lifespan. Moreover, we found that LDPE possesses a tensile strength of 15 MPa, which indicates their robustness and ability to withstand external forces, making them highly resistant to wear and tear. This strength ensures the product remains durable even under stressful conditions, making it suitable for long-term use. By selecting the appropriate material, we have ensured our product's reliability, and our customers can enjoy the benefits of a high-quality, long-lasting product.

J. Wing Manufacturing Plan and weight

During the design phase of the wing assembly, a comprehensive trade study was conducted to compare various types of constructions. Based on the results, a multi-spar type construction was chosen, consisting primarily of three major components: ribs, spars, and skin.

To provide high resistance against bending due to the high moment of inertia about the bending axis, off-the-shelf hollow carbon fiber tubes with a box and circular section were utilized to assemble spars. Carbon fiber tubes are known for their high fatigue strength, which is essential to dampen the deflections caused by a long cantilever beam. Moreover, the highly anisotropic nature of carbon fiber provides excellent suppression of vibrational oscillations caused by bending.

The ribs were cut out of 5mm balsa sheets and spaced equidistantly at 10cm intervals along the wingspan. Additionally, four ribs were placed near the center of the wing to increase its rigidity and structural strength. To enhance the structural capabilities of the ribs, they were further reinforced with a 2mm carbon fiber sheet.

Finally, the wing assembly was completed with a sheeting of monokote, which is a lightweight, heat-shrinkable polyester film widely used in the aerospace industry. The densities used for each of the components, namely the ribs, spars, and skin, are listed in Table 6.

Table 6 Density Values of Wing Components

Component	Density (kg/m ³)
5mm Balsa Sheet	160
2mm CF Sheets	1100
8mm CF Rods	1400
Monokote Sheeting	785

K. Estimation of Free Lift

The Free Lift, denoted by L_{Free} , is a critical parameter in airship design and operation. It is defined as the difference between the Net Static Lift and the Total System Weight, which includes the weight of the Payload. Mathematically, the Free Lift can be obtained using Equation x. A positive value of Free Lift is desirable to accommodate unforeseen circumstances and facilitate altitude gain. To achieve neutral buoyancy, the Free Lift is balanced with the Ballast weight. The Ballast weight can be added or removed as required during the flight to maintain the desired level of Free Lift. Therefore, careful consideration must be given to the determination of Free Lift and Ballast weight during the design phase to ensure safe and stable airship operation.

$$L_{Free} = (L_{env} + L_{wing}) - (W_E + W_{Pay}) \quad (7)$$

VI. Results and Discussion

The design methodology presented earlier has been utilized to size a solar-powered winged hybrid airship that satisfies all the required mission parameters. The sizing process was initiated by defining the values of various assumed operating parameters. These parameters are listed in Table 7 and were carefully selected to ensure a technically sound design that meets the mission requirements. By applying the established design methodology and incorporating the specified operating parameters, the necessary design specifications for the solar-powered winged hybrid airship were determined.

Table 7 Assumed Operational Parameters

Parameter	Symbol	Unit	Value
Operating Altitude	H_{opr}	m	50
Operating velocity	V_{opr}	m/s	15
Average Solar Irradiance	I_{solar}	W/m ²	950

To ensure the technical viability of the solar-powered winged hybrid airship designed for agricultural purposes, it is crucial to carefully consider the ambient air conditions and design constants that will have a significant impact on its performance. At the intended operating altitude of 50m under the International Standard Atmosphere, the temperature, pressure, and density of the ambient air were estimated to be 287.82 K, 100726 N/m², and 1.22 kg/m³, respectively. These values provide critical inputs for the design process. Design constants are parameters that remain constant throughout the design cycle and have a significant impact on the output parameters. They must be carefully chosen based on the specific mission requirements and expected operating conditions. For the design of winged hybrid airships for agricultural purposes, key design constants include the mean sea level density of helium, which is 0.168 kg/m³, as well as various aerodynamic and structural parameters that affect the airship's performance, stability, and control. To ensure a technically sound design, the values of these design constants were obtained from reliable sources, such as [17] and [18], and are listed in Table 8. By incorporating these values into the design process and applying the established design methodology, the necessary design specifications for the winged hybrid airship can be determined, including the required envelope volume, aspect ratio, and lift-to-drag ratio. These design parameters listed in Table 9, in turn, will have a significant impact on the airship's ability to carry out agricultural missions effectively and efficiently, such as monitoring crop health and growth, spraying pesticides or fertilizers, or transporting crops and equipment.

Table 8 Design Constants

Parameter	Unit	Value
Envelope Material Area Density	g/m^2	110
Mass Factor for Joints and patches for envelope	%	5
Tail Material Area Density	g/m^2	200
Mass Factor for Joints and patches for fins	%	3
Solar Panel Area Density	g/m^2	1000
Solar Cell Efficiency	%	12
Battery Energy Density	W-h/kg	595
Propulsion System Energy Density	W/kg	75
Propeller Efficiency	%	85

Table 9 Results of Geometry Sizing

Airship Envelope			
Parameter	Symbol	Units	Value
Volume	V_{env}	m^3	181
Length	l	m	17.85
Maximum Diameter	D_{max}	m	4.2
Profile Cylinder Ratio	a	-	1.2
Fineness Ratio	FR	-	4.25
Surface Area	S_{surf}	m^2	199
Reference Area	$Vol^{2/3}$	m^2	32
Wing Planform			
Wingspan	b_w	m	4.5
Chord	c_w	m	0.5
Aspect Ratio	AR_w	-	9
Coefficient of Lift	C_L	-	1.02
Coefficient of Drag	C_D	-	0.113
Tailplane $\times 4$			
Tailspan	b_t	m	1.40
Root chord	c_{rt}	m	2.48
Tip chord	c_{tt}	m	1.75
Surface Area	S_t	m^2	2.95
Aspect Ratio	AR_t	-	0.66

The results of Lift, Drag, and Power computation are listed in Table 10.

Table 10 Results of Lift, Drag and Power computations

Parameter	Unit	Value
Net Static Lift _{airship}	N	1865.60
Wing Lift	N	280.86
Volumetric Drag Coefficient _{airship}	-	0.0321
Drag coefficient _{wing}	-	0.021
Drag force or Thrust required	N	217.78
Required Propulsive Power	W	3843.21
Total Power Required	W	3943.21
Required Solar Panel Area	m ²	34.59

A. Vehicle Mass Estimation

Vehicle mass is a critical factor in airship design that directly impacts the vehicle's stability and maneuverability. The weight of the winged airship is distributed across its various components such as the envelope, gondola, propulsion system, and payload, and can be represented in Equation 8.

$$M_{tot} = M_{env} + M_{fin} + M_{wing} + M_{solar} + M_{propulsion} + M_{payload} + M_{battery} + M_{gondola} \quad (8)$$

Proper weight distribution is essential to ensure that the vehicle remains stable and level during flight. The distribution of weight is also crucial to maintain the center of gravity within acceptable limits, as this directly affects the vehicle's ability to maneuver and change direction. The estimation of envelope and fin mass can be obtained by calculating their material properties and dimensions and utilizing the provided gram per square meter (gsm) value to determine their mass based on these parameters. As for the wing, its mass can be estimated by determining its dimensions and material properties and applying established formulas or simulation tools. The weight of the gondola was determined using its dimensions and density. The payload mass is a predetermined parameter for the mission and is thus already known, encompassing all scientific instruments, communication equipment, or other items that will be transported on the spacecraft. The solar panel mass can be estimated by utilizing their area density, which involves determining the solar panel dimensions and the density of the material they are made of. The propulsion system and battery weight are calculated by using their respective parameters as mentioned in Table 11.

The weight breakdown of the solar-powered wing hybrid airship meeting the specified mission requirements is listed in Table 11 and shown in the form of a Pie Chart in Figure 11.

Table 11 System Weight Breakdown

Component	Weight (kg)
Envelope	22.96
Wing	8
Tailplane	2.43
Solar Panels	4.5
Propulsion System	52.58
Batteries	88.36
Gondola	5.62
Payload	30
Free Lift (Ballast)	4.34
Total Weight	218.8

From the results, it is apparent that for solar-powered winged hybrid airships designed for agricultural purposes, the battery and propulsion system components constitute the maximum weight of the vehicle. However, due to the high lift

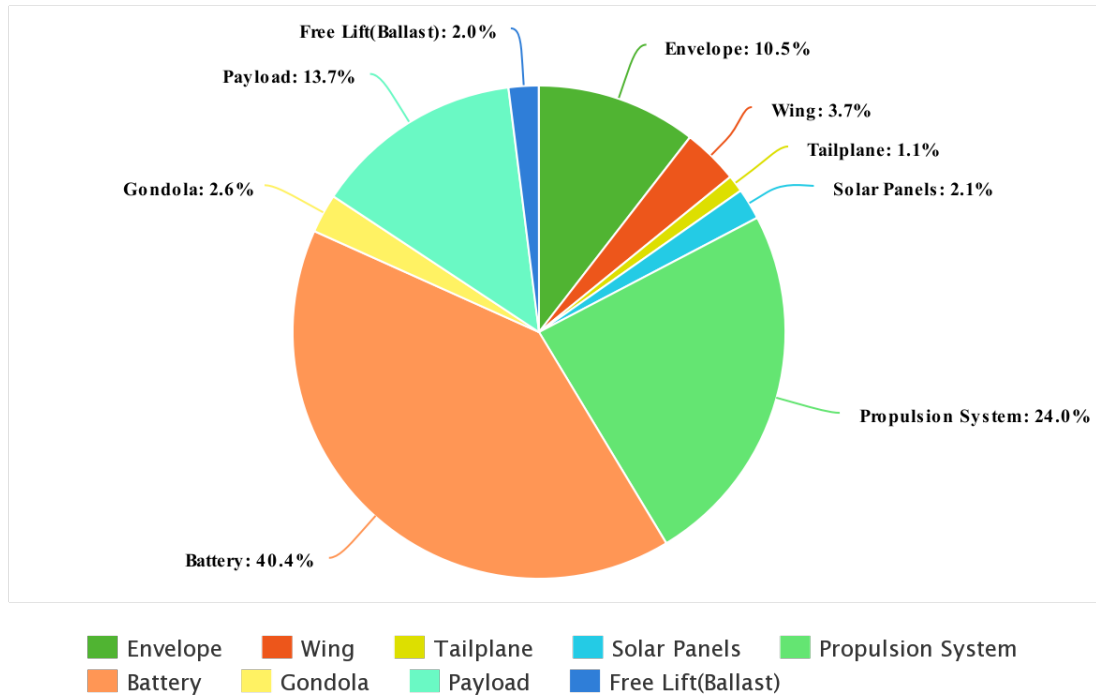


Fig. 11 Weight breakdown of the system

generated by the airfoil and the power generation capacity of the solar panels, the vehicle is able to carry a sizeable payload of 30 kg while maintaining an endurance of 24 hours. The ability to carry a payload for an extended period makes the vehicle suitable for a range of agricultural applications, including crop monitoring, mapping, and surveying. Additionally, the solar-powered propulsion system makes the vehicle an eco-friendly alternative to conventional aerial vehicles, making it a promising solution for sustainable agriculture. Figure 12 shows the final CAD model of the solar-powered winged hybrid airship.

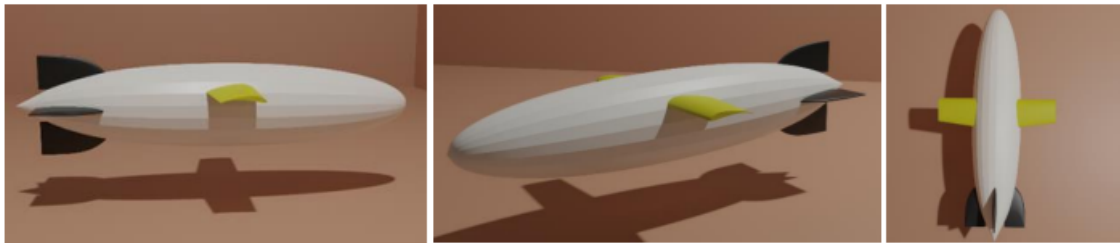


Fig. 12 Final CAD geometry of the solar-powered winged hybrid airship

VII. Conclusions

The purpose of this paper is to present the conceptual design and sizing of a solar-powered winged hybrid airship for agricultural applications. The study concludes that an airship is a viable vehicle configuration for agricultural purposes. The battery is the heaviest component of the airship, but it can be optimized further to enhance the vehicle's endurance. During the study, an endurance of 24 hours was achieved while keeping the weight of the airship under 200 kg.

Future work on this design will include the optimization of various design parameters and a detailed sensitivity analysis to determine the correlation between different design outputs. This design offers superior performance parameters and is capable of successfully accomplishing the mission.

The proposed solar-powered winged hybrid airship has demonstrated its potential as an efficient and reliable platform for agricultural applications. The lightweight design, combined with the use of solar power, makes it an environmentally friendly solution for farmers. With the ability to cover a large area and gather data in real time, this airship can provide valuable insights to farmers, leading to improved crop yields and reduced costs. Overall, this study presents a promising design that has the potential to revolutionize the agricultural industry.

References

- [1] "Agricultural land (% of land area)," <https://data.worldbank.org/indicator/AG.LND.AGRI.ZS>, 2021. Accessed on May 2, 2023.
- [2] Srinivasan, K. V., *Drones for Precision Agriculture*, The Institution of Engineers (India), 2016.
- [3] McBratney, A., Whelan, B., and Ancev, T., "Future directions of precision agriculture," *Precision Agriculture*, Vol. 6, 2005, pp. 7–23.
- [4] Katin, O., and Belozarov, V., "Advantages of using an Agro-fire Airship for solving problems of Agriculture and Fire Protection," *European Journal of Natural History*, 2021.
- [5] Maniyamkott, M. J., "Drone Crop Surveys to Ease Farmers' Lives," *Indian Express*, 2015.
- [6] Puri, V., Nayyar, A., and Raja, L., "Agriculture drones: A modern breakthrough in precision agriculture," *Journal of Statistics and Management Systems*, Vol. 20, No. 4, 2017, pp. 507–518.
- [7] Kleemann, N., Karpuk, S., and Elham, A., "Conceptual Design and Optimization of a Solar-Electric Blended Wing Body Aircraft for General Aviation," *AIAA Scitech 2020 Forum*, 2020, p. 0008.
- [8] Kersten, T., Wolf, J., and Lindstaedt, M., "Investigations Into the Accuracy of the Uav System Dji Matrice 300 Rtk with the Sensors Zenmuse p1 and II in the Hamburg Test Field," *XXIV ISPRS Congress "Imaging today, foreseeing tomorrow"*, 6–11 June 2022, Nice, France, Copernicus, 2022, pp. 339–346.
- [9] Sato, A., "The rmax helicopter uav," Tech. rep., YAMAHA MOTOR CO LTD IWATA (JAPAN) FUNDAMENTAL RESEARCH DIV, 2003.
- [10] Sakamoto, T., Ogawa, D., Hiura, S., and Iwasaki, N., "Alternative procedure to improve the positioning accuracy of orthomosaic images acquired with agisoft metashape and DJI P4 multispectral for crop growth observation," *Photogrammetric Engineering & Remote Sensing*, Vol. 88, No. 5, 2022, pp. 323–332.
- [11] Kurakov, F., "The Economics of Science," *The Economics of Science*, Vol. 3, No. 3, 2017, pp. 214–226. <https://doi.org/10.22394/2410-132X-2017-3-3-214-226>.
- [12] Prentice, B. E., and Knotts, R., "Cargo airships: international competition," *Journal of Transportation Technologies*, Vol. 2014, 2014.
- [13] Nayler, A., "Airship development world-wide-A 2001 review," *1st AIAA, Aircraft, Technology Integration, and Operations Forum*, 2013, p. 5263.
- [14] Poirion, F., and Mortchelewicz, G., "Airship gust response probabilistic model construction," *EURODYN 2020*, 2020.
- [15] Mistri, S. R., and Pant, R. S., "Design and fabrication of a quick dismantlable remotely controlled semirigid finless airship," *Innovative Design and Development Practices in Aerospace and Automotive Engineering: I-DAD, February 22-24, 2016*, Springer, 2017, pp. 103–116.
- [16] Xavier, E., "XFLR-5 Software," <http://www.xflr5.com/>, 2021.
- [17] Carichner, G. E., and Nicolai, L. M., *Fundamentals of Aircraft and Airship Design: Volume 2—Airship Design and Case Studies*, American Institute of Aeronautics and Astronautics, Inc., 2013.
- [18] Alam, M. I., and Pant, R. S., "Multi-objective multidisciplinary design analyses and optimization of high altitude airships," *Aerospace science and technology*, Vol. 78, 2018, pp. 248–259.